Title: New families of single integration vectors and gene tagging plasmids for genetic manipulations in budding yeast.
Authors: Wosika V, Durandau E, Varidel C, Aymoz D, Schmitt M, Pelet S
Journal: Molecular genetics and genomics : MGG
Year: 2016 Dec
Volume: 291
Issue: 6
Pages: 2231-2240
DOI: 10.1007/s00438-016-1249-1

New families of Single Integration Vectors and Gene Tagging plasmids for genetic manipulations in budding yeast

Victoria Wosika, Eric Durandau, Clémence Varidel, Delphine Aymoz, Marta Schmitt and Serge Pelet*

Department of Fundamental Microbiology, University of Lausanne, Switzerland

*Corresponding Author: serge.pelet@unil.ch; phone +41 21 692 5621

Abstract

The tractability of the budding yeast genome has provided many insights into the fundamental mechanisms regulating cellular life. With the advent of synthetic biology and single-cell measurements, novel tools are required to manipulate the yeast genome in a more controlled manner. We present here a new family of yeast shuttle vectors called Single Integration Vectors (pSIV). Upon transformation in yeast, these plasmids replace the entire deficient auxotrophy marker locus by a cassette containing an exogenous marker. As shown using flow cytometry, this complete replacement results in a unique integration of the desired DNA fragment at the marker locus. In addition, a second transcriptional unit can be inserted to achieve the simultaneous integration of two constructs. The selection marker cassettes, present in the pSIV, were also used to generate a complete set of gene tagging plasmids encompassing a large palette of fluorescent proteins, from a Cyan Fluorescent Protein (CFP) to a near-infrared tandem dimer Red Fluorescent Protein (tdiRFP). These tagging cassettes are orthogonal to each other thanks to the use of different TEF promoter and terminator couples thereby avoiding marker cassette switching and favoring integration in the desired locus. In summary, we have created two sets of robust molecular tools for the precise genetic manipulation of the budding yeast.

Keywords: plasmid, integration, gene tagging, fluorescent protein, transformation, molecular biology, genetic modification, yeast expression

Introduction

Pioneer model organism in the study of eukaryotic cells, *Saccharomyces cerevisiae* has contributed to the understanding of many cellular mechanisms such as cell-cycle regulation, cell polarity, signal transduction, metabolism or aging (Drubin and Nelson 1996; Nasmyth 1996; Chen and Thorner 2007; Cai and Tu 2012; Longo et al. 2012). This important role in fundamental biology can be attributed in a large part to the variety of tools developed to manipulate the yeast genome (Botstein et al. 1997; Gietz and Woods 2006; Botstein and Fink 2011). The generation of genome-wide collections of ORF deletions or ORF-GFP tagged strains are two excellent illustrations of this ability (Winzeler et al. 1999; Huh et al. 2003).

Shuttle vectors, allowing the transfer of cloning plasmids directly from a bacterial host to a yeast strain, have also participated in the success of *S.cerevisiae* as a eukaryotic model system. A standard set of plasmids (pRS) with four auxotrophy markers for *HIS3*, *LEU2*, *TRP1* and *URA3* is widely used in the yeast community (Sikorski and Hieter 1989). Three variants of these plasmids are available: two-micron, centromeric and integrative. Two-micron plasmids are high copy number plasmids used for the over-expression of proteins. Centromeric plasmids possess an autonomously replicating sequence (ARS) allowing them to be replicated at each cell cycle and segregated between mother and daughter cells. For these constructs, the average number of plasmids per cell in the population is around one. However, at the single-cell level, some yeast contains two copies of the plasmid while others have lost it. Finally, integrative plasmids are directly inserted into the yeast genome via homologous recombination at a specific locus. This generates an evident uniformity between sister cells bearing the plasmids since they are isogenic. Moreover, the insert can be maintained at its locus even in absence of selection.

Centromeric plasmids have been used successfully in countless studies, where responses were measured at the population level. In the last decade, with the development of single-cell studies and synthetic biology, a need has emerged to control precisely the genetic information in each individual cell. The integrative plasmids have thus gained in importance. The stable integration in the host genome allows a more uniform expression of the exogenous construct in each cell of the population. This can be crucial for synthetic gene regulatory circuits where each part of the network has to be expressed at a stable and defined level (Cantone et al. 2009). Studies in the transcription field also require the stable integration of expression reporters in order to assess noise in gene expression. Indeed, the presence of multiple copies will alter the characterization of the variability in expression or will change the measured rate of protein expression.

Unfortunately, the standard pRS integrative plasmids have a large tendency to integrate multiple times at the same locus. In this paper, we have designed a new family of shuttle vectors that integrate only once thanks to a complete replacement of the deficient auxotrophy locus. We assessed the efficiency of unique integration of our plasmids against the standard pRS vectors by yeast transformation and flow cytometry analysis of the transformants fluorescence. Additionally, using the same auxotrophy cassettes, we generated a complete set of gene tagging plasmids comprising five commonly used fluorescent proteins, thus covering a large spectral range from blue to near-infrared.

Materials and methods

Strains and plasmids
All experiments were performed in W303 background. Yeast strains are listed in Table S1. The Single Integration Vector URA (pSIVu) was constructed by Gibson Assembly (Gibson Assembly Master Mix, New England BioLabs) of PCR amplified fragments (Microsynth) and synthetized DNA geneblocks (Integrated DNA technologies) with overlapping compatible tails. The Single Integration Vectors LEU (pSIVl), HIS (pSIVh) and TRP (pSIVt) were constructed by restriction digest of pSIVu with PacI to retrieve the bacterial part (Fig. 2a white part) and ligating it with synthetic DNA fragments (Biomatik) bearing the synthetized yeast part sequences, either coming from a different yeast species or codon shuffled *in silico* (Table 1).

For the FACS analysis, the same construction (p*PRS2*-mCherry-t*SIF2*) was inserted into a standard pRS306 plasmid and the newly designed Single Integration Vector URA (pSIVu). Additionally, in the pSIV vector, we inserted a second transcriptional unit in the MCS2 encoding for a double green fluorescent protein (p*TEF*-PP7-2xGFP-t*CYC1*). This construct was first cloned in the minimal plasmid (pMCV) and subsequently cloned with AatII-SphI into the pSIV. Thes plasmids are listed in Table S2

Transformants generation and flow cytometry analysis
Chemically competent cells were generated from a culture of W303 wild type strain (ySP2) following standard protocol (Gietz and Woods 2006) and transformed with either 1.5µg of EcoRV linearized pRS vector (pVW110) or 1.5µg of PacI linearized pSIV vector (pVW169) and plated on SD-URA selection plates. Four replicates were performed in parallel, leading to four transformation plates per vector. After three days of growth at 30 °C, twenty-four transformants were randomly picked from each transformation plate and streaked on a new selection plate for one day of growth. All isolated transformants were then grown overnight in 200µL selective medium to saturation in 96 well plates (Greiner CELLSTAR 96 M9311-100EA). The next morning, cells were diluted 40-fold into 200 µl of non-selective medium (SD-Full) and analyzed by flow cytometry after at least four hours of growth.

Samples were loaded as 96 well plates with the High Throughput Sampler into an LSRFortessa flow cytometer (BD Biosciences). Red and green fluorescently tagged histones strains were used as fluorescence positive controls. Isolated versus clustered cells were separated by a gating based on FSC and SSC values of a sonicated WT culture. Measurements were acquired for 10'000 recorded events in the defined gate or 100 seconds. For the red fluorescence, samples were excited with a 561 nm yellow-green laser and the fluorescence emission was detected through a 610/20 nm filter. Green fluorescence was measured by exciting with a 488 nm blue laser and detected with a 530/30 nm filter.

Flow cytometry data were analyzed with Matlab (The MathWorks). A gating on the FSC and SSC was applied to select the single cell events. Only 6 samples out of 192 had fewer than 8'000 events in the gate. The fluorescence of these samples was within the expected distribution of the population suggesting that they were less concentrated due to low inoculation or small dilution issues during sample preparation. Definition of the single integrant status was performed by setting low and high thresholds for the median fluorescence value of the sample. For the pSIV, the difference between the lowest and highest single integration transformant is 750. For the pRS, we added 500 to the lowest transformant intensity above background to set the high fluorescence threshold.

Gene tagging and transformation
Gene tagging primers were designed with consensus forward and reverse sequences annealing to all pGT vectors (Fig. 4a blue primers): 5'-GCGGCCGCTCTAGAACTA-3' and 5'-ATGGAAAAACGCCAGCAACG-3'respectivelly, to which a gene specific sequence of 40 bp was flanked and used for the homologous recombination with the C-terminus of the targeted ORF. Table S3 lists all the primers used in this study. Gene tagging PCRs were run as 50 µl reaction at an annealing temperature of 65 °C (30s), with an extension time of 2 min (72 °) for all pGTs, using a high-fidelity enzyme (Q5 High-Fidelity polymerase, New England Biolabs). After a gel electrophoresis control of the PCR specificity, 20µl of PCR reaction were used to transform the cells following a standard lithium acetate protocol (Gietz and Woods 2006).

Microscopy
Images were acquired on an inverted epi-fluorescence microscope (Ti-Eclipse, Nikon) controlled by micro-manager (Edelstein et al. 2010), with a 60X oil objective and excitation and emission filters: CFP, YFP, RFP and iRFP. The excitation light is provided by a solid-state light source (SpectraX, Lumencor) and the images were recorded with an sCMOS camera (Flash4.0, Hamamatsu) with the following exposure times: CFP (100ms), YFP (300ms) RFP (100 ms) iRFP (100 ms). Log-phase yeast cultures were diluted to OD 0.04, briefly sonicated and 200 µl of culture were loaded in a well coated with ConcanavalinA (0.5 mg/ml, C2010-250MG, Sigma-Aldrich). Cells were stressed by addition of 100 µl of SD-full NaCl 1.2M in the well to a final concentration of 0.4M NaCl.

All pSIV and pGT plasmids presented in this study will be made available on Addgene. Their accession numbers are provided in Table 1 and Table 2.

Results

pRS integration
The integration of the vectors from the pRS family requires a linearization of the backbone by enzymatic restriction in the selection marker. In the W303 background, auxotrophy for all selection markers is due to deficient marker genes, with one or two point mutations (*leu2-3,112; trp1-1; ura3-1; his3-11,15*) (Ralser et al. 2012). Homologous recombination can be obtained by digestion of the pRS plasmid within the ORF of the marker. In BY4741, there is a complete deletion of the auxotrophy ORFs (*his3*Δ, *leu2*Δ and *ura3*Δ) (Brachmann et al. 1998). Integration of the pRS vectors is performed by cutting either in the promoter or the terminator of the marker to obtain homology regions with the corresponding genomic sequence. In either case, the integration of a wild type sequence restores the prototrophy of the targeted gene thanks to a duplication of the genomic region upon integration (Fig. 1a). These two sequences can in turn serve as recombination sites for other transformed DNA molecules, possibly leading to multiple integrations. Therefore, transformants have to be screened for single integration of the vector. This screening process can be relatively straightforward in the case of a fluorescent construct. However, genotyping by PCR is typically difficult due to the large size of the plasmid backbone. Alternatively, single versus multiple integrations can be verified by qPCR or Southern blots.

Single Integration Vector architecture
The solution to this multiple integration issue is rather simple and can be achieved by having two sites of homology at the 5' and 3'-ends of the integrating cassette such that the entire

locus is replaced at each integration event (Fig. 1b). This implies, however, that the auxotrophy marker should not have any homology with the endogenous locus to prevent recombination at wrong sites. To this purpose, we synthetized four exogenous auxotrophy cassettes (Table 1). For the *URA3* and *HIS3* loci, we used the *C. albicans* and *S. pombe* homologs, respectively, which were already used in the gene tagging plasmids (pKT, (Sheff and Thorn 2004)). For *LEU2* and *TRP1*, we scrambled the endogenous *S. cerevisiae* sequence to preserve the amino acid order while randomizing the codon usage and considering the codon bias of the budding yeast. We also optimized the DNA sequence to remove the most commonly used restriction sites. Similarly to a large family of gene deletion plasmids (Wach et al. 1997; Longtine et al. 1998), we used TEF promoters and terminators to control the expression of these four markers (Steiner and Philippsen 1994). In order to avoid marker switch when transforming successively multiple pSIV plasmids in the same strain, we used four different combinations of p*TEF* and t*TEF* from close relative yeast species (Table 1). We verified by growth curve and spot assays that these new markers can sustain growth in selective and non-selective media (Supp. Fig. 1). To have the ability to recycle some selection markers, we inserted inverted *loxP* sites (Fig. 2a) at each side of the markers to offer the possibility to loop out the marker using the Cre recombinase (Sauer 1987).

The homology with the genomic DNA is based on two 250 bp regions in the promoter and terminator of the marker gene (Table 1). The sequence in the promoter region was selected upstream of the transcription start site based on tiling array data (David et al. 2006), in order to prevent the production of transcripts arising from the genomic promoter inside the plasmid. Upstream of the promoter and downstream of the terminator homology regions, two restriction sites for PacI and BstBI have been inserted. As it can be seen on the map of the pSIV vector on Figure 2a, digestion of the plasmid with either of one of these restriction enzymes will generate two fragments. One half contains the yeast integrative element (green elements in Fig. 2a) and the other contains all the sequences required for the plasmid amplification in bacteria. In opposition to what happens with the pRS plasmid, this bacterial part will not be integrated in the yeast genome, which reduces the size of the integrated DNA.

A multiple cloning site (MCS) is present downstream of the TEF terminator (Fig. 2a). This MCS contains all the sites present in the MCS of the standard pBLUESCRIPT or pRS vectors (Sikorski and Hieter 1989). The sequences of the vector have been optimized in order to ensure that each one of these sites is unique. Because it is often necessary to introduce multiple constructs in one strain, we created the possibility to integrate a second MCS, between the unique restriction sites AatII and SphI, which are positioned upstream of the TEF promoter. For this purpose, we generated a MCS2 cloning vector (pMCV) containing the bacterial part from the pSIV and a standard MCS flanked by AatII and SphI that we call MCS2 (Fig. 2b). The second construct can be assembled in this minimal plasmid, sequence verified and sub-cloned into the pSIV. Note that since the MCS1 and MCS2 contain the same restriction sites, insertion of the second MCS often leads to a duplication of many sites. Sequences annealing to the standard sequencing primers T3/T7 and M13forward/reverse were inserted on each side of the MCS1 and MCS2, respectively, allowing independent sequencing of each MCS.

Verification of single insertion into the genome

To compare the efficiency of the pSIV and pRS plasmids to generate single integration transformants, we cloned a red fluorescent protein (RFP) variant mCherry under the control of the constitutive promoter p*RPS2* in a pSIV URA3 (pSIVu) and in a pRS URA3 (pRS306). A

similar amount of these two backbones was linearized by restriction digest (respectively PacI and EcoRV). Without purification, the entire restriction digestion mix was added to chemically competent W303 wild type cells following standard transformation protocol (Giesecke et al. 2006).

After three days of growth on SD-URA plates, twenty-four single colonies from each transformation were streaked on selective plates. They were then grown overnight in 96-well plates in liquid medium to saturation, diluted 40 fold and grown for 4 hours before the fluorescence of individual cells was measured by flow cytometry. Figure 3a represents the histogram of the fluorescence of more than eight thousand cells for ten pSIV transformants. All the curves show an almost complete overlap. In comparison, the ten transformants bearing the pRS plasmid display a large variability in fluorescence levels (Fig. 3b). The median fluorescence intensities of the 24 selected colonies are plotted in increasing order for the four replicates (Fig. 3c and 3d). Out of the total 96 colonies screened for the pSIV, only two of them display an aberrant fluorescence level. One is non-fluorescent, the other one is 6-times brighter than the other clones (Figure 3c). The picture is strikingly different with the pRS plasmid, where the clones cover a large range of fluorescence (Figure 3d). In both cases, we defined a range of fluorescence intensity that we consider as single integration transformants. For the pSIV, 98% of the clones fell in this range, while only 12.5% can be considered to have a single integration for the pRS transformation. The rest of them are false positives (23%) or multiple integrations (64.5%) (Fig. 3e).

Correlation of MCS1 and MCS2 integration

In order to verify if the MCS1 and the MCS2 present on the pSIV plasmid integrate with the same efficiency in the genome, the pSIV vector with the p*RPS2*-mCherry construct also contained a p*TEF* 2xGFP inserted in the MCS2. The fluorescence intensity of the pSIV transformants was scored simultaneously in the red and green channels of the flow cytometer (Fig. 3f). Out of the 96 clones, three outliers were found: the two previously measured clones with no RFP and very high RFP intensities, plus one additional strain that has a normal RFP level but displays a two-fold higher GFP intensity. Overall this analysis suggests that the simultaneous transformation of both MCSs is the most likely outcome.

Development of a complete set of gene tagging plasmids

In parallel to plasmid integration, the ability to tag genes directly with fluorescent proteins has provided many insights into the localization and function of yeast proteins (van Drogen et al. 2001; Maeder et al. 2007; Cai et al. 2008; Pelet et al. 2011). Moreover, it is often desirable to tag simultaneously multiple proteins in the same cells to correlate their location. The pKT plasmids are widely used in the yeast community to tag proteins with various fluorescent spectral variants. However, only two auxotrophy markers (HIS and URA) and one antibiotic resistance (KAN) are available for selection of the positive transformants. In addition, the same TEF promoter and terminator are used for all these cassettes. This increases the chances of inducing a marker exchange rather than the correct insertion of a second fluorescent tag at the desired locus.

In order to allow the tagging of four different proteins, each with a different fluorescent tag, we decided to use the auxotrophy marker generated for the pSIV plasmids and create a family of gene tagging plasmids (pGT) that covers the spectrum of commonly used FPs from CFP to iRFP (Table 2). For the CFP channel, we used the yeast enhanced monomeric variant of CFP (yemCFP) (Sheff and Thorn 2004). In the YFP channel, the mCitrine variant was used because of its higher photostability compared to the faster maturing Venus. Note that two

mutations (A206K, L221K) are used to render it monomeric (Zacharias et al. 2002; Sheff and Thorn 2004). The superfolder GFP (sfGFP) was chosen due to its brightness, fast maturation and a recognized ability to tag proteins that are usually difficult to render fluorescent (Pédelacq et al. 2006). We selected the RFP variant mCherry due to its brightness and photostability (Shaner et al. 2004). In the far-red region of the spectrum, we use the tandem dimer infrared FP (tdiRFP) (Filonov et al. 2011). This protein has a relatively low brightness compared to other FPs, and should mostly be used to tag abundant proteins. In order to facilitate the PCR amplification of this tandem dimer protein, we codon shuffled the coding sequence of the second copy of the iRFP.

All monomeric fluorescent proteins are cloned between XbaI and XhoI sites, allowing an easy exchange of the tagging peptide, which could be newer versions of FP or protein affinity tags for biochemistry experiments (Fig. 4a). An *ADH* terminator is placed downstream of the fluorescent protein sequence. As in the pSIV, *lox*P sites flank the marker cassette to excise and recycle it for other genetic manipulations.

To test the efficient tagging of pGT plasmids and their orthogonality, we used all four markers to tag four proteins inside the same cell: Pma1-yemCFP:*URA3* (membranes), Dcp2-mCitrine:*LEU2* (P-bodies), Hog1-mCherry:*TRP1* (cytoplasm and nucleus) and Hta2-tdiRFP:*HIS3* (nucleus). Cells were imaged before and after a hyper-osmotic shock. This stress leads to the accumulation of Hog1 in the nucleus (Reiser et al. 1999) and the formation of P-bodies (Teixeira et al. 2005) (Fig. 4b).

Discussion

In this study, we developed two sets of plasmids for precise genetic manipulation of the budding yeast based on optimized auxotrophy markers. Theses non-endogenous cassettes were then used to build four shuttle vectors that only integrate once into the genome (pSIVs, Table 1) and new gene tagging plasmids (pGTs, Table 2). The presence of a different set of promoter and terminator for each one of the markers allows an orthogonality within the pGTs and pSIVs within a single cell and increases the efficiency of correct genetic integrations during yeast transformation.

To demonstrate the unique genomic integration of the Single Integration Vectors (pSIVs), we scored the number of single integrations against the standard pRS vectors. As expected, pSIV transformation led to a clearly improved homogeneity between the transformants, compared to pRS transformants. Surprisingly, the low RFP fluorescence intensity range that we attributed to single integration events was not the same for both types of transformants. The single integration threshold for the pSIV plasmids was set higher than for the pRS vectors (Fig. 3c and 3d dashed blue lines). The fact that virtually all pSIV transformants displayed the same fluorescence intensity strongly hinted that they were single integration clones. In order to verify that single integration was the predominant form of integration of the pSIV plasmid, we transformed an empty plasmid and verified by PCR on genomic locus the size of the inserted cassette using forward and reverse primers outside of the integration region (Supp Fig. 2). The eleven transformants tested displayed the expected band at 2.2kb versus 1.5kb for the endogenous URA3 locus in the mother strain. Thus, the discrepancy in fluorescence intensity between pSIV and pRS plasmids is not due to multiple integrations of the pSIV. A more likely explanation of this difference resides in the backbone composition. Terminators are known to play a key role in mRNA stability and therefore in controlling the steady-state

level of protein expression. Our red fluorescent construct carries a *SIF2* terminator, which has been described to be of intermediate strength (Yamanishi et al. 2013). Thus, if not all transcription is terminated within the 500bp of the terminator, the sequence directly following this terminator could influence the stability of the mRNA and thereby explain the difference between pSIV and pRS transformants intensities.

Because there is only a handful of available selection markers, a second insert can be cloned between AatII and SphI in the pSIVs, with an intermediate cloning step into a specifically designed MCS2 cloning vector (Fig. 1b). The two transcriptional units can be expressed and integrated within the same plasmid. Care must be taken, however, when designing the plasmid, to avoid large homology regions between the two inserts. These similar DNA sequences could perturb the whole replacement of the cassette when multiple successive homologous recombinations happen in the same cell.

In summary, pSIVs transformation provides a clearly improved reliability in generating single integration transformants. Combined integration of the two MCSs happens in an overwhelming majority of cases. Despite this great fidelity, individual transformants have to be screened. However, the number of transformants to screen is reduced to a minimum, allowing to perform directly a deeper phenotypic analysis of each one of these few clones. In comparison, the pRS plasmid transformation generates a great diversity in fluorescence expression levels, which renders careful screening processes essential and time-consuming. It has to be noted that the amount of plasmid transformed and the competency of the cells will strongly influence the output of this transformation. Reducing the amount of plasmid tends to decrease the number of multiple integrations in the final clones. In each one of the four pRS transformations performed, we identified at least one single integration clone, but the large diversity in fluorescence intensity makes it difficult to set the threshold with high precision.

To conclude, we described here four new non-endogenous transcriptional units expressing auxotrophy markers for the design of a set of Single Integration Vectors (pSIV) and their derivative Gene Tagging plasmids (pGT). In comparison to the standard yeast shuffle pRS vectors, which integrate inside the coding sequence of selection markers, pSIV plasmids integrate into the host genome thanks to two homology sequences: the first one in the promoter and the second one in the terminator of the auxotrophy locus. This complete exchange of the deficient gene by an exogenous DNA fragment leads to a single integration of the vector. In comparison, the pRS plasmids integrate multiple times because of the duplication of the marker locus. We demonstrated these behaviors by quantifying the integration of a fluorescent protein construct using flow cytometry. Moreover, thanks to this mechanism of integration, pSIVs can be applied identically for transformation in the two most commonly used *S. cerevisiae* backgrounds W303 and BY4741. In addition, using the same four auxotrophy markers, we constructed a complete family of gene tagging plasmids for the fluorescent labeling of endogenous proteins. We tagged four different proteins in the same cell with different FP spectral variants demonstrating that pGTs can be used in parallel to visualize multiple proteins in the same strain, thanks to their orthogonality. All the plasmids described here are available on Addgene together with their sequences.

Acknowledgements

We thank all members of the Pelet and Martin labs for helpful discussions, Barbara Brandani for technical assistance and Paul Majcherczyk for the support with the FACS machine.

Author contributions

SP, VW, DA and ED designed the experiments. VW, DA and MS constructed and tested the pSIV plasmids. ED and CV constructed and tested the pGT library. VW performed the flow cytometry and microscopy experiments. SP and VW analyzed the data and wrote the manuscript.

Compliance with ethical standards

Funding. This study was supported by SystemsX.ch (IPhD 51PHP0_157354) and Swiss National Science Foundation grants (PP00P3_139121) and the University of Lausanne.

Conflict of interest. All authors declare that they have no conflict of interest.

Ethical approval. This article does not contain any studies with human participants or animals performed by any of the authors.

References

Botstein D, Chervitz SA, Cherry JM (1997) Yeast as a model organism. Science 277:1259–1260.

Botstein D, Fink GR (2011) Yeast: an experimental organism for 21st Century biology. Genetics 189:695–704.

Brachmann CB, Davies A, Cost GJ, Caputo E, Li J, Hieter P, Boeke JD (1998) Designer deletion strains derived from Saccharomyces cerevisiae S288C: a useful set of strains and plasmids for PCR-mediated gene disruption and other applications. Yeast 14:115–132.

Cai L, Dalal CK, Elowitz MB (2008) Frequency-modulated nuclear localization bursts coordinate gene regulation. Nature 455:485–490.

Cai L, Tu BP (2012) Driving the cell cycle through metabolism. Annu Rev Cell Dev Biol 28:59–87.

Cantone I, Marucci L, Iorio F, Ricci MA, Belcastro V, Bansal M, Santini S, di Bernardo M, di Bernardo D, Cosma MP (2009) A yeast synthetic network for in vivo assessment of reverse-engineering and modeling approaches. Cell 137:172–181.

Chen RE, Thorner J (2007) Function and regulation in MAPK signaling pathways: lessons learned from the yeast Saccharomyces cerevisiae. Biochim Biophys Acta 1773:1311–1340.

David L, Huber W, Granovskaia M, Toedling J, Palm CJ, Bofkin L, Jones T, Davis RW, Steinmetz LM (2006) A high-resolution map of transcription in the yeast genome. Proc Natl Acad Sci USA 103:5320–5325.

Drubin DG, Nelson WJ (1996) Origins of cell polarity. Cell 84:335–344.

Edelstein A, Amodaj N, Hoover K, Vale R, Stuurman N (2010) Computer control of microscopes using μManager. Curr Protoc Mol Biol Chapter 14:Unit14.20.

Filonov GS, Piatkevich KD, Ting L-M, Zhang J, Kim K, Verkhusha VV (2011) Bright and stable near-infrared fluorescent protein for in vivo imaging. Nat Biotechnol 29:759–763.

Giesecke AV, Fang R, Joung JK (2006) Synthetic protein–protein interaction domains created by shuffling Cys2His2 zinc-fingers. Molecular Systems Biology. doi: 10.1038/msb4100053

Gietz RD, Woods RA (2006) Yeast transformation by the LiAc/SS Carrier DNA/PEG method. Methods Mol Biol 313:107–120.

Huh W-K, Falvo JV, Gerke LC, Carroll AS, Howson RW, Weissman JS, O'Shea EK (2003) Global analysis of protein localization in budding yeast. Nature 425:686–691.

Longo VD, Shadel GS, Kaeberlein M, Kennedy B (2012) Replicative and chronological aging in Saccharomyces cerevisiae. Cell Metab 16:18–31.

Longtine MS, McKenzie A, Demarini DJ, Shah NG, Wach A, Brachat A, Philippsen P, Pringle JR (1998) Additional modules for versatile and economical PCR-based gene deletion and modification in Saccharomyces cerevisiae. Yeast 14:953–961.

Maeder CI, Hink MA, Kinkhabwala A, Mayr R, Bastiaens PIH, Knop M (2007) Spatial regulation of Fus3 MAP kinase activity through a reaction-diffusion mechanism in yeast pheromone signalling. Nat Cell Biol 9:1319–1326.

Nasmyth K (1996) At the heart of the budding yeast cell cycle. Trends in Genetics 12:405–412.

Pelet S, Rudolf F, Nadal-Ribelles M, de Nadal E, Posas F, Peter M (2011) Transient activation of the HOG MAPK pathway regulates bimodal gene expression. Science 332:732–735.

Pédelacq J-D, Cabantous S, Tran T, Terwilliger TC, Waldo GS (2006) Engineering and characterization of a superfolder green fluorescent protein. Nat Biotechnol 24:79–88.

Ralser M, Kuhl H, Ralser M, Werber M, Lehrach H, Breitenbach M, Timmermann B (2012) The Saccharomyces cerevisiae W303-K6001 cross-platform genome sequence: insights into ancestry and physiology of a laboratory mutt. Open Biol 2:120093.

Reiser V, Ruis H, Ammerer G (1999) Kinase activity-dependent nuclear export opposes stress-induced nuclear accumulation and retention of Hog1 mitogen-activated protein kinase in the budding yeast Saccharomyces cerevisiae. Mol Biol Cell 10:1147–1161.

Sauer B (1987) Functional expression of the cre-lox site-specific recombination system in the yeast Saccharomyces cerevisiae. Mol Cell Biol 7:2087–2096.

Shaner NC, Campbell RE, Steinbach PA, Giepmans BNG, Palmer AE, Tsien RY (2004) Improved monomeric red, orange and yellow fluorescent proteins derived from Discosoma sp. red fluorescent protein. Nat Biotechnol 22:1567–1572.

Sheff MA, Thorn KS (2004) Optimized cassettes for fluorescent protein tagging in Saccharomyces cerevisiae. Yeast 21:661–670.

Sikorski RS, Hieter P (1989) A system of shuttle vectors and yeast host strains designed for efficient manipulation of DNA in Saccharomyces cerevisiae. Genetics 122:19–27.

Steiner S, Philippsen P (1994) Sequence and promoter analysis of the highly expressed TEF gene of the filamentous fungus Ashbya gossypii. Mol Gen Genet 242:263–271.

Teixeira D, Sheth U, Valencia-Sanchez MA, Brengues M, Parker R (2005) Processing bodies require RNA for assembly and contain nontranslating mRNAs. RNA 11:371–382.

van Drogen F, Stucke VM, Jorritsma G, Peter M (2001) MAP kinase dynamics in response to pheromones in budding yeast. Nat Cell Biol 3:1051–1059.

Wach A, Brachat A, Alberti-Segui C, Rebischung C, Philippsen P (1997) Heterologous HIS3 marker and GFP reporter modules for PCR-targeting in Saccharomyces cerevisiae. Yeast 13:1065–1075.

Winzeler EA, Shoemaker DD, Astromoff A, et al (1999) Functional characterization of the S. cerevisiae genome by gene deletion and parallel analysis. Science 285:901–906.

Yamanishi M, Ito Y, Kintaka R, Imamura C, Katahira S, Ikeuchi A, Moriya H, Matsuyama T (2013) A Genome-Wide Activity Assessment of Terminator Regions in Saccharomyces cerevisiaeProvides a ″Terminatome″ Toolbox. ACS Synth Biol 2:337–347.

Zacharias DA, Violin JD, Newton AC, Tsien RY (2002) Partitioning of lipid-modified monomeric GFPs into membrane microdomains of live cells.

Figure Legends

Figure 1. Integration mechanism of pRS vectors compared to Single Integration Vectors a. Scheme describing the integration of a pRS plasmid at the marker locus. The first integration event duplicates the marker generating one functional and one non-functional copy of the auxotrophy marker. Subsequent homologous recombination events will result in further multiplication of the marker and MCSs. **b.** Integration of the pSIV in the auxotrophy locus by homologous recombination with the promoter and terminator regions (pLOC, tLOC). The complete replacement of the locus results in a single MCS being integrated even if multiple successive homologous recombination events take place.

Figure 2. Map of the Single Integration Vector. a. The vector is composed of two parts, the bacterial part (white) and the yeast part (green). The expression of the marker is controlled by a *TEF* promoter and terminator couple. The homologous recombination occurs via the homology regions pLOCUS and tLOCUS. The MCS1 is composed of a set of unique restriction sites. A second MCS can be inserted between the AatII and SphI sites. **b.** Map of the MCS2 cloning vector composed only of the bacterial part and an MCS1 flanked by AatII and SphI for sub-cloning into the pSIV.

Figure 3. Comparison of the single integration efficiency for pSIV and pRS vectors. a. and **b.** Histograms of the RFP fluorescence of 10 transformants bearing the pSIV (a) and the pRS backbone (b). The insets in each panel describe the integrated construct. **c.** and **d.** Median RFP fluorescence intensities of 24 transformants obtained from four independent transformations of the pSIV (c) or the pRS (d) vectors. The colonies were sorted according to their median intensity level. The dashed lines delimit the intensity intervals considered as single integration transformants. **e.** Percentages of false positives, single integrations and multiple integrations for the transformation of the two different backbones. **f.** Correlation between RFP and GFP intensities in the 96 transformants quantified by flow cytometry. The inset is a blown-up of the region where the large majority of the clones are found.

Figure 4. Four colour tagging of a yeast strain using the pGT cassettes. a. Schematic of the gene tagging cassette. **b.** Images of cells bearing four fluorescent proteins imaged before and after (20 min) stress with 0.4M NaCl. Hta2-tdiRFP stains the nucleus. Pma1-CFP localizes at the plasma membrane and the vacuole. Hog1-mCherry translocates in the nucleus after stimulus. The aggregation of P-bodies induced by the stress can be visualized by local enrichments of Dcp2-mCitrine.

Tables

Table 1: pSIV markers information

Marker	Gene origin	pTEF species	tTEF species	Marker coordinates	pMARKER coordinates	tMARKER coordinates	Marker size (bp)	Addgene ID
URA3	*C. albicans* Ura3	*A. gossypii*	*A.gossypii*	116167-116970 (chr. V)	116067-115815	116791-117041	1420	**81089**
LEU2	*S. cerevisiae* Leu2 scr.	*S. kudriavzevii*	*C.glabrata*	91324-92418 (chr.III)	90980-91230	92450-92700	1845	**81090**
HIS3	*S. pombe* His5	*S. kudriavzevii*	*A.gossypii*	721946-722608 (chr.XV)	721650-721900	722630-722880	1382	**81091**
TRP1	*S. cerevisiae* Trp1 scr.	*A. gossypii*	*C.glabrata*	461842-462516 (chr.IV)	461350-461600	462530-462780	1306	**81092**

scr: scrambled, chr : chromosome, p: promoter, t: terminator
Marker size includes the pTEF, the marker and the tTEF sequences.

Table 2: Gene tagging plasmids (pGT) set

Marker	yemCFP	sfGFP	mCitrine	mCherry	tdiRFP
URA3	GTU-c (81093)	GTU-g (81094)	GTU-y (81095)	GTU-r (81096)	GTU-ir (81097)
LEU2	GTL-c (81098)	GTL-g (81099)	GTL-y (81100)	GTL-r (81195)	GTL-ir (81102)
HIS3	GTH-c (81103)	GTH-g (81104)	GTH-y (81105)	GTH-r (81106)	GTH-ir (81107)
TRP1	GTT-c (81108)	GTT-g (81109)	GTT-y (81110)	GTT-r (81111)	GTT-ir (81112)

GT: gene tagging, c: cyan, g: green, y: yellow, r: red, ir: infrared, (Addgene ID).

Figure 1:

a.

pRS Integrative Plasmids

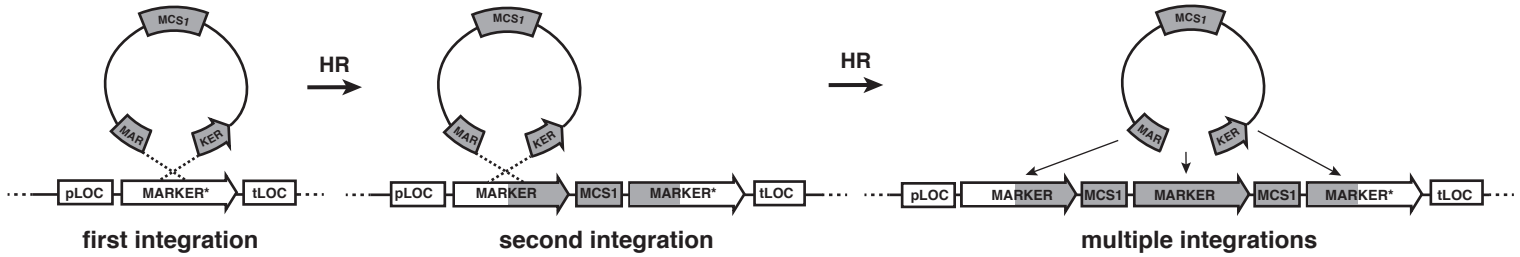

b.

Single Integration Vectors

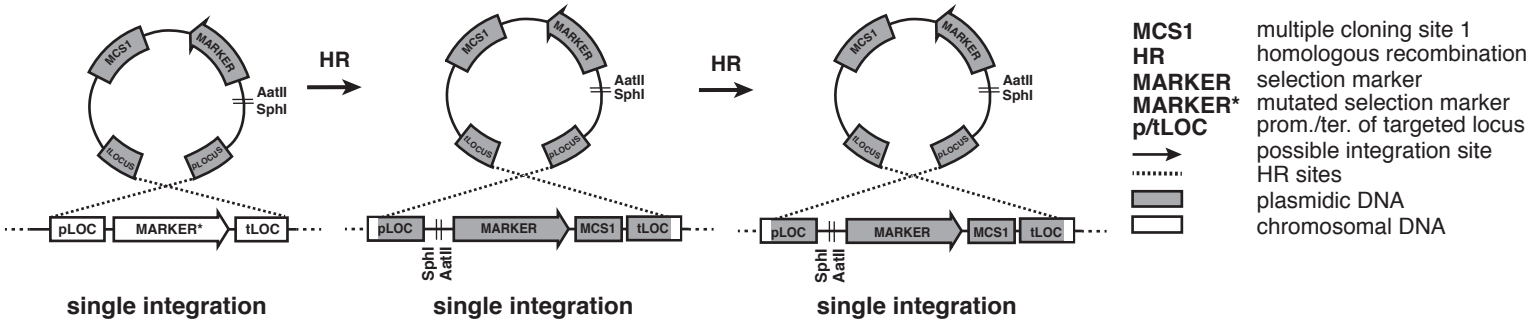

Figure 2:

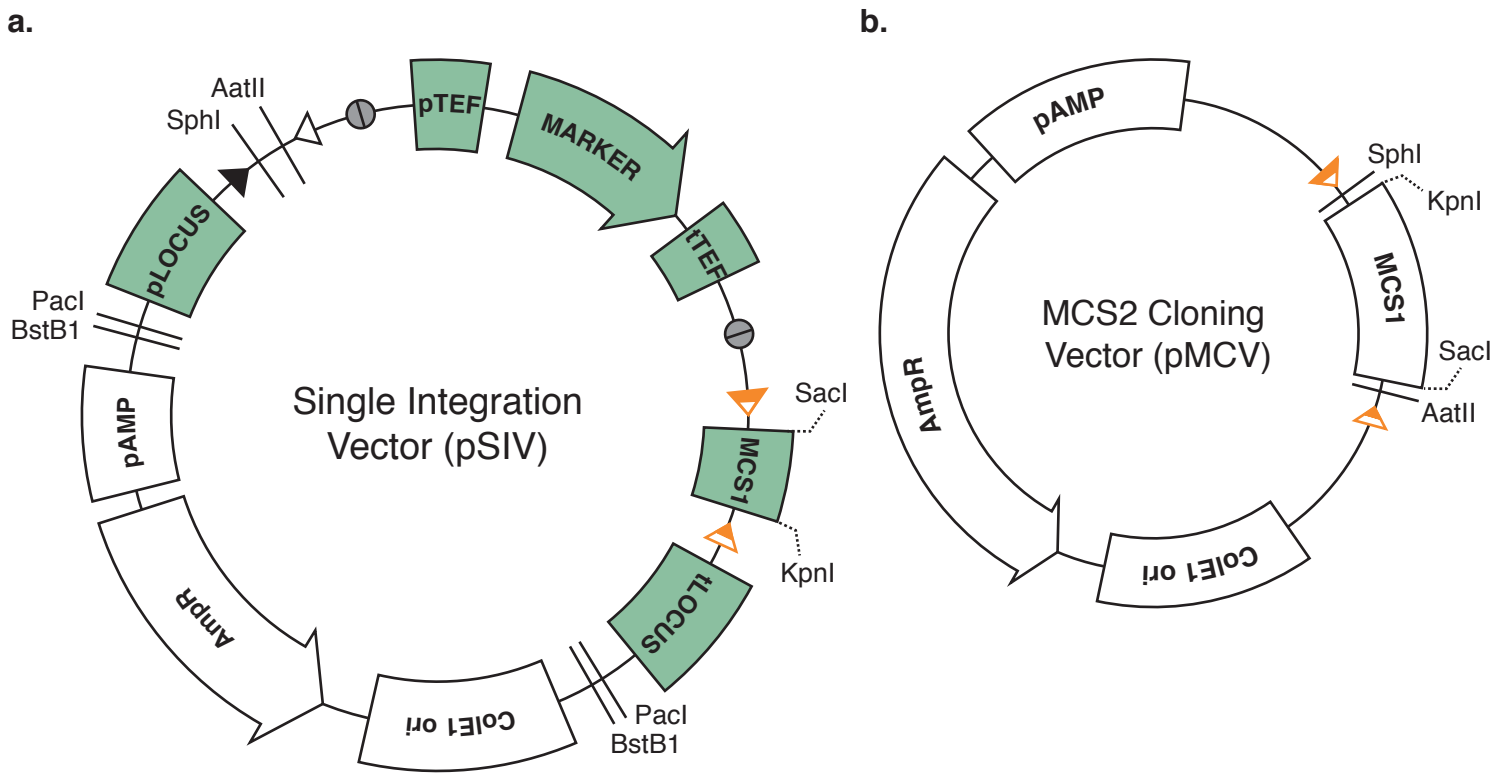

m13fw/m13rev T7/T3 loxP sites

MCS1: SacI SacII XbaI BamHI PstI EcoRV ClaI XhoI KpnI
BstXI EagI SpeI SmaI EcoRI HindIII SalI ApaI

MCS2: AatII-MCS1-SphI

Figure 3:

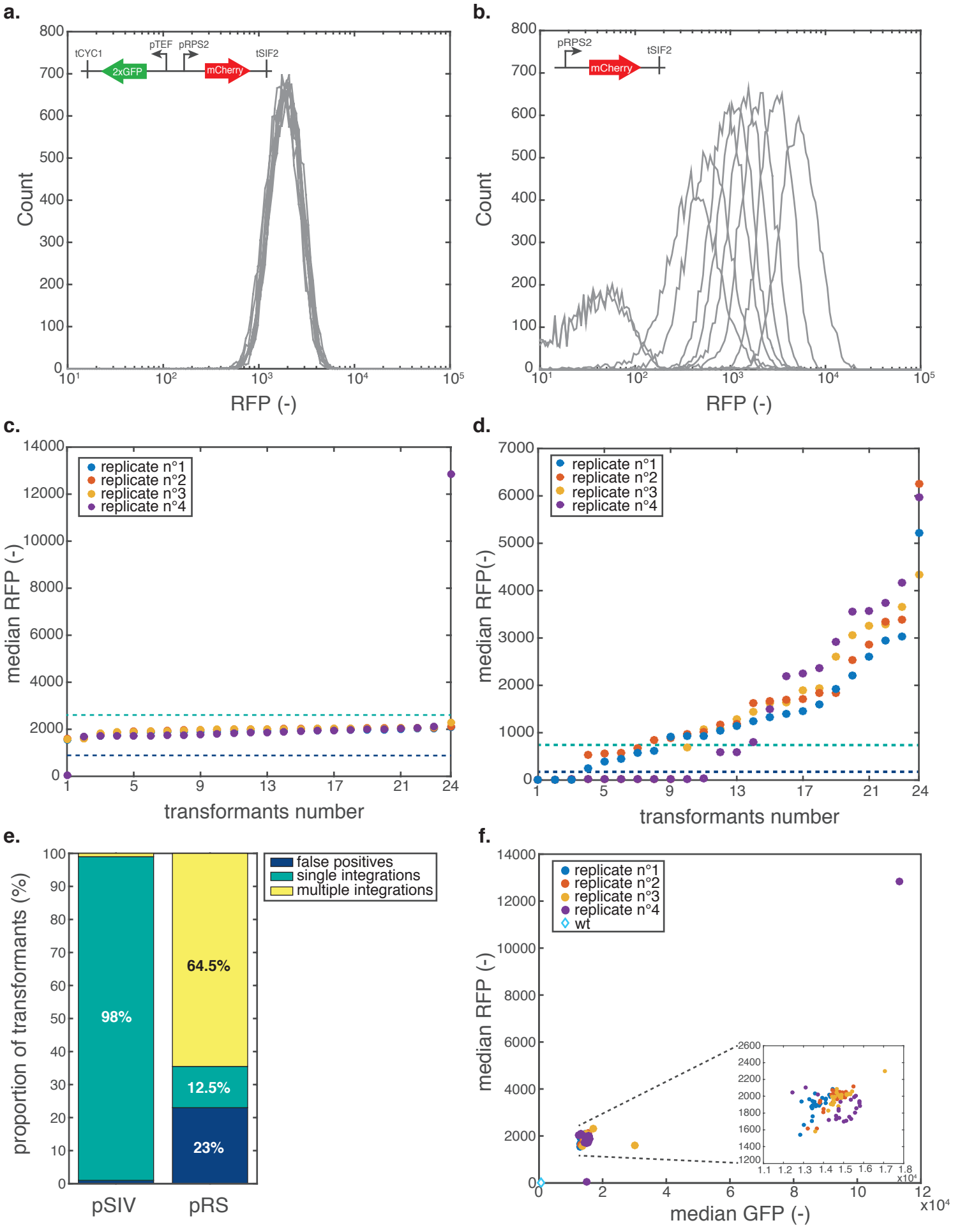
a.
tCYC1
2xGFP
pTEF
pRPS2
mCherry
tSIF2
Count
RFP (-)
b.
pRPS2
mCherry
tSIF2
Count
RFP (-)
c.
replicate n°1
replicate n°2
replicate n°3
replicate n°4
median RFP (-)
transformants number
d.
replicate n°1
replicate n°2
replicate n°3
replicate n°4
median RFP(-)
transformants number
e.
false positives
single integrations
multiple integrations
proportion of transformants (%)
98%
64.5%
12.5%
23%
pSIV
pRS
f.
replicate n°1
replicate n°2
replicate n°3
replicate n°4
wt
median RFP (-)
median GFP (-)
x10⁴

Figure 4:

a.

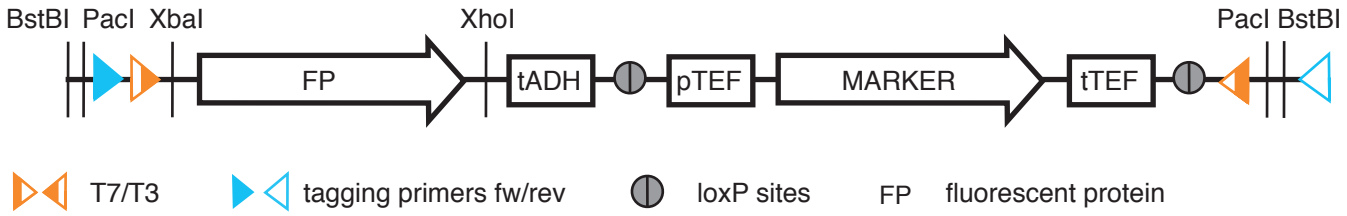
BstBI
PacI
XbaI
XhoI
PacI
BstBI
FP
tADH
pTEF
MARKER
tTEF
T7/T3
tagging primers fw/rev
loxP sites
FP
fluorescent protein

b.

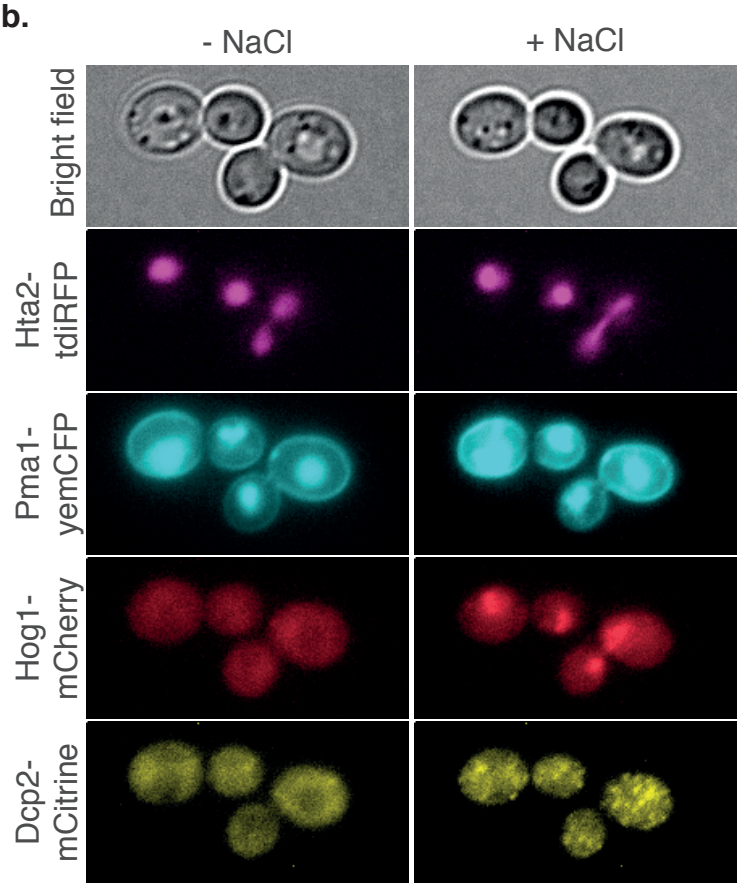
- NaCl
+ NaCl
Bright field
Hta2-tdiRFP
Pma1-yemCFP
Hog1-mCherry
Dcp2-mCitrine

Supplementary Figure 1:

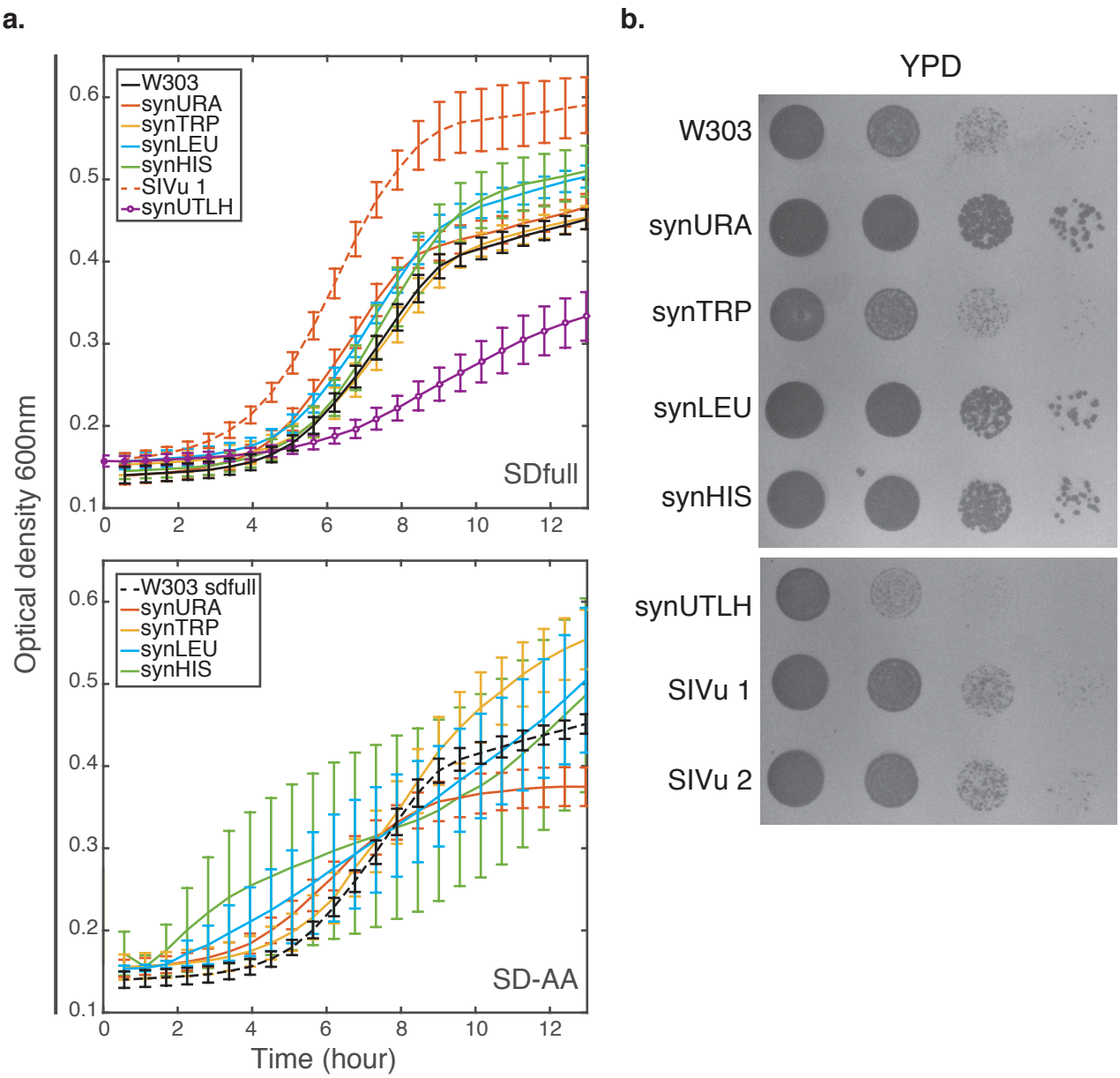

Supplementary Figure 1: Integration of the synthetic marker cassettes in the genome has little influence growth rate. a) Growth curves of *hta2*-mCherry pGT tagged strains bearing each of the four marker cassettes, compared to the wt W303 background, the four colors tagged strain from Fig. 4b and a pSIVu clone from Fig 3, in SDfull and selective medium (SD-AA, except WT). The curves represent the mean and standart deviation of 8 replicates automatically measured every 30 min in a 96 wells plate by a Tecan Infinite microplate reader (Tecan Group Ltd, Männedorf, Switzerland), starting from an OD600 0.1 diluted overnight culture. **(b)** Spot assay performed with the same cultures as the growth assay. Cells were initially diluted to $1.26x10^7$ cells (first column) and then followed by 1/10 serial dilutions.

Supplementary Figure 2: **Genotyping pSIV transformants for single integration**

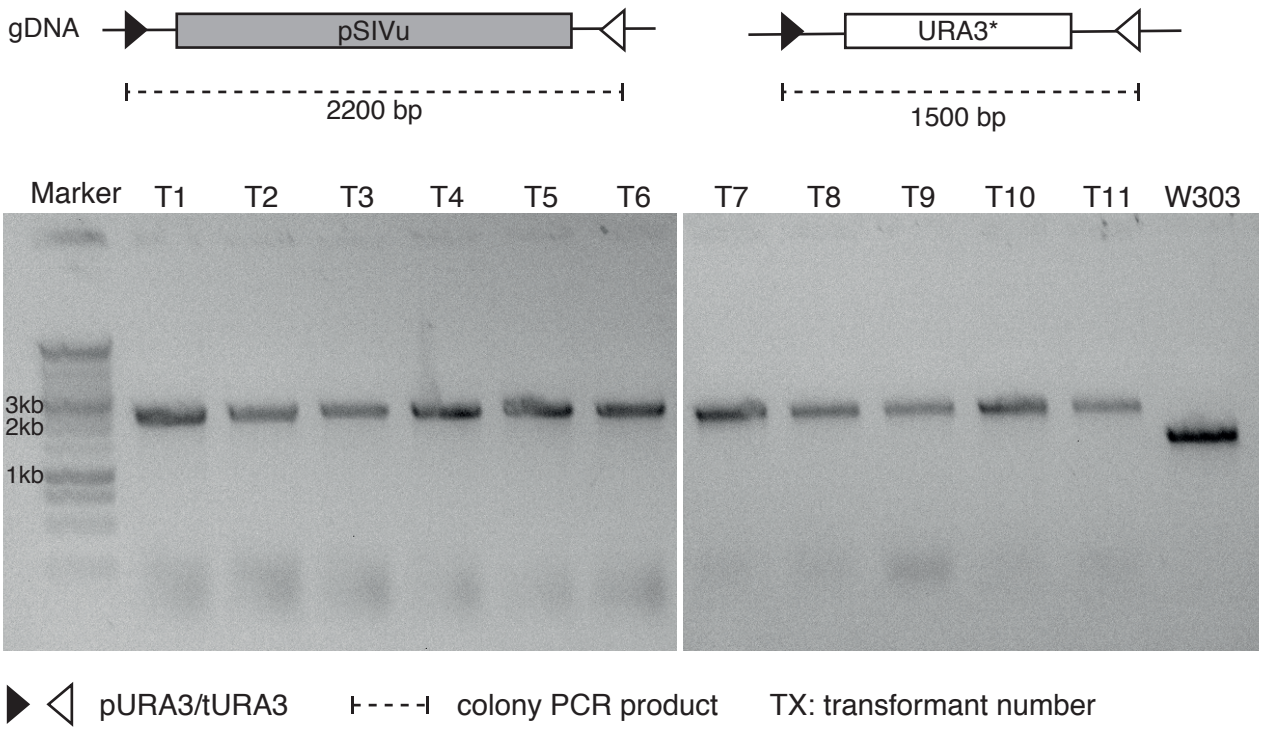

Supplementary Figure 2: Colony PCR to confirm the single integration of the pSIVu plasmid. Scheme showing the location of the primers (sequence found in Table S3) on the genomic DNA used for genotyping the presence and number of integrated plasmids (grey box) versus the endogenous locus (white box), and the expected PCR product size. Compared to the mother strain, all eleven transformants returned a band of 2.2 kb corresponding to the single integration of the empty plasmid, as shown in the agarose gel.

Supplementary Table S1: Strains used in this study

Yeasts	Genotype	Resistance
ySP2	*MAT*a {*leu2-3,112 trp1-1 can1-100 ura3-1 ade2-1 his3-11,15*}	-
yVW81	*w303 pRPS2 mCherry tSIF2*	U
yVW82	*w303 pRPS2 mCherry tSIF2 pTEF PP7 2xGFP tCYC1*	U
yVW140	*w303 hta2-iRFP:HIS dcp2-mCitrine:LEU hog1-RFP:TRP pma1-yemCFP:URA*	UHTL

ySP2: W303 naked background. U: URA3 resistance. UHLT: URA3, TRP1, LEU2 and HIS3 resistance

Supplementary Table S2: Plasmids used in this study

Plasmids	Insert	Selection
pVW110	pRS306 *pRPS2 mCherry tSIF2*	URA
pVW169	pSIVu *pRPS2 mCherry tSIF2 pTEF PP7 2xGFP tCYC1*	URA

Supplementary Table S3: Primer sequences

Primer name	5'-3' Sequence
pURA3	agaaaaggattaaagatgctaagagatag
tURA3	actcttgttgttctttggagttca
T3	AATTAACCCTCACTAAAGGG
T7	TAATACGACTCACTATAGGG
M13fw	TGTAAAACGACGGCCAGT
M13rev	CAGGAAACAGCTATGACCATG
pGT fw	GCGGCCGCTCTAGAACTA
pGT rev	ATGGAAAAACGCCAGCAACG
Dcp2 fw	cgaatggaacttcagggtctaatgaattattaagcattttgcataggaagGCGGCCGCTCTAGAACTA
Dcp2 rev	tcaaattgtgttatggttgtttaatcttattgaataccagtatcaaggatATGGAAAAACGCCAGCAACG
Hog1 fw	cggtaaccaggccatacagtacgctaatgagttccaacagGCGGCCGCTCTAGAACTA
Hog1 rev	gctgataaacaaacaatacgccataagtgacggttcttggATGGAAAAACGCCAGCAACG
Pma1 fw	acttcatggctgctatgcaaagagtctctactcaacacgaaaaggaaaccGCGGCCGCTCTAGAACTA
Pma1 rev	agttgattaaaatgtgacaaaaattatgattaaatgctacttcaacaggaATGGAAAAACGCCAGCAACG
Hta2 fw	acttgttgccaaagaagtctgccaagactgccaaagcttctcaagaactgGCGGCCGCTCTAGAACTA
Hta2 rev	cgtaacaaaagaaagagagcctagctgtaatatatctttataacatgtatATGGAAAAACGCCAGCAACG

Capital letter: plasmid-annealing sequence. Lower case: sequence annealing to genomic DNA.